

Supplementary Information (SI)

Unique assemble of carbonylpyridinium and chromene reveal mitochondrial thiol starvation under ferroptosis and novel ferroptosis inducers

Kaiqing Ma,^a He Yang,^a Tianruo Shen,^c Yongkang Yue,^a Lingling Zhao,^a Xiaogang Liu,^c
Fangjun Huo,^b Caixia Yin ^{a*}

a Key Laboratory of Chemical Biology and Molecular Engineering of Ministry of Education, Institute of Molecular Science, Shanxi University, Taiyuan 030006, PR China

E-mail: yincx@sxu.edu.cn

b Research Institute of Applied Chemistry, Shanxi University, Taiyuan 030006, PR China

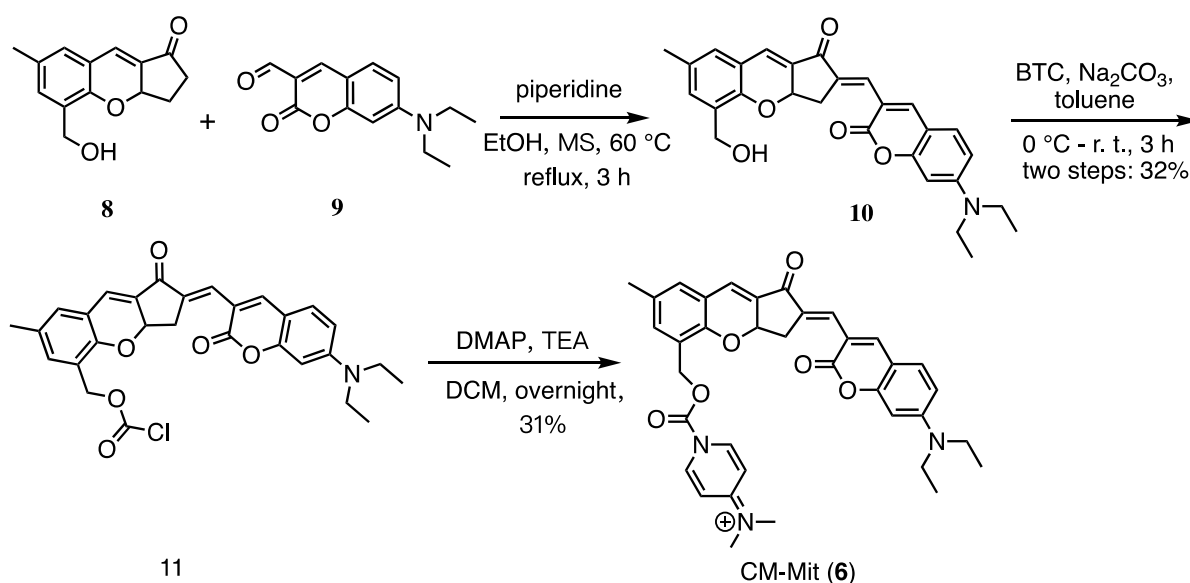
c Singapore University of Technology and Design, 487372, Singapore

Table of contents

| |
|-----------------------|
| 1. Experiment Section |
| 2. Additional Figures |
| 3. NMR and MS Spectra |
| 4. Reference |

Experiment Section

Materials and Chemicals. The commercial chemicals were used without further purification. Distilled water was obtained after passing through a water ultra-purification system. TLC analysis was performed using commercial silica plates. Fluorescence spectra were recorded on Hitachi F-7000 fluorescence spectrophotometer. Hitachi U-3900UV-vis spectrophotometer was used to measure UV-vis spectra. ^1H NMR and ^{13}C NMR experiments were conducted with a BRUKER AVANCE III HD 600 MHz and 151 MHz NMR spectrometer, respectively. (Bruker, Billerica, MA). Coupling constants (J values) are reported in hertz. HRMS determinations were recorded on a Thermo Scientific Q Exactive Instruments. An IVIS spectrum imaging system (PerkinElmer) was employed for bioluminescent imaging in animal.



Scheme S1. The synthesis of Probe **CM-Mit**

Synthesis of probe CM-Mit Compound **8** and **9** were synthesized according to the procedure reported by our group previously [1-3].

Synthesis of compound **11**:

To a solution of compound **8** (200 mg, 0.87 mmol) and compound **9** (255.6 mg, 1.04 mmol) in 3 ml ethanol were added piperidine dropwise in seal tube under argon. The resulting mixture was stirred at 60 °C for 3 h. The mixture was concentrated to afford the crude product **3**, which was submitted to the next reaction directly.

To the solution of the crude product in toluene (3 ml) were added BTC (561.1 mg, 1.74 mmol) and sodium carbonate (118.6 μL , 1.74 mmol) at 0 °C. The resulting

mixture was stirred at room temperature for 3 h under argon. The mixture was concentrated and purified on a silica gel column (PE/EA/DCM = 4:1:1) to afford the desired product **11** 144 mg in 32% yield for two steps.

Synthesis of compound **6**:

To a solution of compound **11** (80 mg, 0.15 mmol) in 0.6 ml DCM were added DMAP (183 mg, 1.5 mmol) and TEA (2 μ L, 0.18 mmol). The resulting mixture was stirred at room temperature overnight and concentrated to afford the residue, which was further purified on a silica gel column (DCM/CH₃OH = 20:1) to afford 31 mg the desired product **6** in 31% yield.

¹H NMR (600 MHz, DMSO-d₆) δ 8.35 (d, J = 7.3 Hz, 1H), 8.25 (s, 0H), 7.67 (d, J = 9.0 Hz, 0H), 7.53 (d, J = 2.7 Hz, 0H), 7.39 (d, J = 2.4 Hz, 0H), 7.37 – 7.31 (m, 0H), 7.21 (d, J = 2.1 Hz, 0H), 7.05 (d, J = 7.3 Hz, 1H), 6.81 (dd, J = 9.0, 2.4 Hz, 0H), 6.60 (d, J = 2.4 Hz, 0H), 5.37 (s, 1H), 5.32 (ddd, J = 8.8, 6.4, 2.6 Hz, 1H), 3.50 (d, J = 7.2 Hz, 2H), 3.17 (s, 3H), 2.25 (s, 1H), 1.15 (t, J = 7.0 Hz, 3H). ¹³C NMR (151 MHz, DMSO) δ 189.3, 162.8, 161.5, 156.8, 156.3, 152.3, 151.1, 144.0, 142.7, 136.1, 134.8, 133.2, 132.0, 131.7, 131.6, 130.1, 128.0, 127.3, 123.5, 123.3, 114.1, 110.3, 108.9, 108.3, 96.9, 74.5, 55.3, 44.8, 36.3, 34.9, 29.2, 29.1, 22.6, 20.5, 14.4, 12.9. HRMS (ESI) [M^+] calculated for C₃₁H₃₂N₃O₄S: 606.2599, found: 606.2553;

Optical Studies of Probe CM-Mit. DMSO (analytical grade) was used to prepare the probe **CM-Mit** (2 mM/L) stock solutions. The stock solutions of analytes (20 mM/L) were afforded in distilled water. The desired concentrations were obtained by the dilution of the stock solutions of analytes with distilled water. In a typical measurement, probe **CM-Mit** (5 μ M) was added to 2 mL of dimethyl sulfoxide/phosphate- buffered saline (DMSO/PBS) (v/v, 1:1, pH = 7.4) in a quartz cell. The UV-vis or fluorescent spectra were then recorded upon addition of analytes at 25 °C.

Imaging in the Living Cells. The HeLa cells were cultured at 37 °C in the 1 \times SPP medium (1% protease peptone, 0.2% glucose, 0.1% yeast extract, 0.003% EDTA ferric sodium salt). In the culture media, HeLa cells were incubated with 10 μ M/L of probe **CM-Mit** (DMSO stock solution) for 30 min at 37 °C, followed by washing with PBS. At the same time, another section of cells was pretreated with N-methylmaleimide (NEM: 200 μ M/L), followed by incubation with probe **CM-Mit** (40 μ M/L, DMSO stock solution) for 30 min at 37 °C. After washing with PBS buffer, the cells were imaged.

Computational Methods. Density functional theory (DFT) and time-dependent DFT (TD-DFT) based calculations were performed in Gaussian 16 program [4-6]. All the calculations were computed using ω B97XD functional and def2-SVP basis set in water [7-8]. We checked the values of frequencies to confirm the geometric structures are optimized to the local minimum in the ground and excited states. We considered the solvent effects using the SMD solvent model and corrected linear-response (cLR) solvent formalism for the soft scans of potential energy surfaces (PES) [9-10]. The molecular structures and orbitals were visualized in Avogadro using the outputs from Gaussian 16[11].

In Vivo Fluorescence Images of Endogenous Thiols. Isoflurane was employed to anesthetize the mice, which were maintained in an anesthetized state for imaging. The probe **CM-Mit** (100 μ M) was injected subcutaneously into the mice, followed by imaging using an IVIS imaging system with a 598 nm excitation and an emission filter of 690 ± 10 nm and images collected at 0, 2, 4, 6, 10, and 20 min, respectively.

Additional Figures

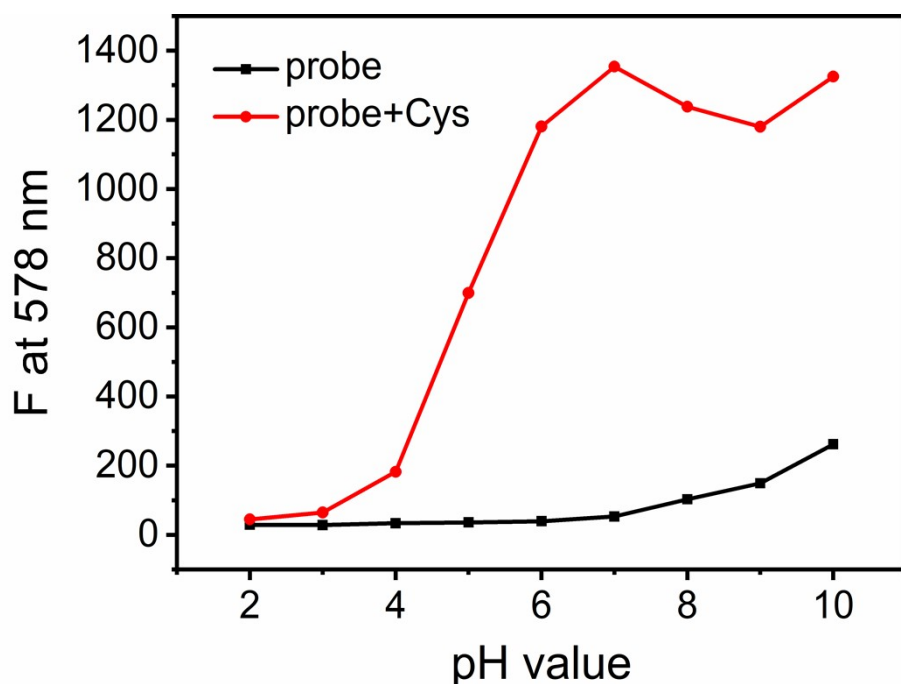


Figure S1: Fluorescent intensity changes of CM-Mit (5 μM) and extra addition of Cys (200 μM) in a mixed solvent of DMSO and PBS (1:9, v/v) after 5 min at various pH values.

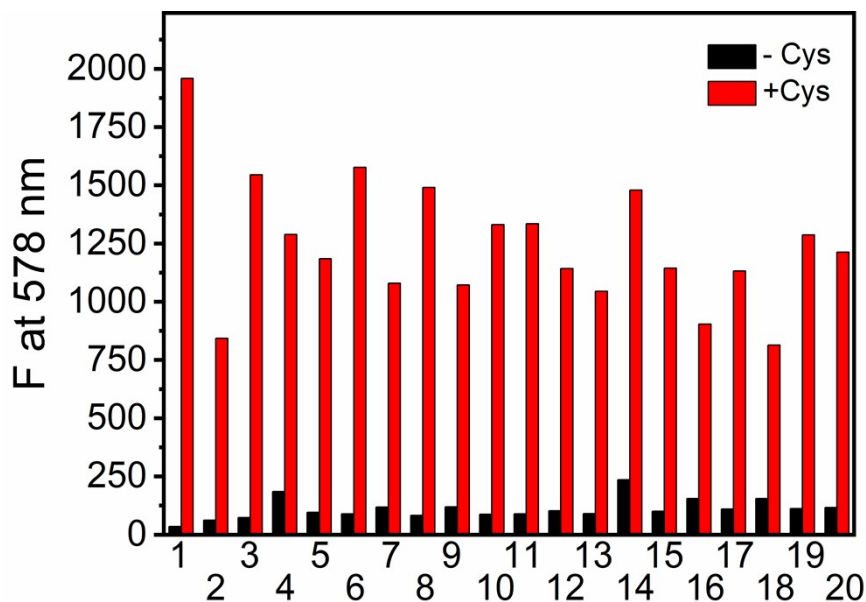


Figure S2: Fluorescent intensity responses of **CM-Mit** (5 μM , DMSO: PBS, 1: 9, v/v) to various ions after 5 min at 578 nm. Including: 1 is the blank group, 2 to 20 represent 1 mM Br⁻, Na⁺, CO₃²⁻, HCO₃⁻, K⁺, NH₄⁺, SCN⁻, OH⁻, F⁻, Mg²⁺, Ca²⁺, SO₄²⁻, Fe²⁺, Fe³⁺, Al³⁺, NO₂⁻, Zn²⁺, H₂O₂, ClO⁻, respectively. Black and red columns indicate no or extra addition of 200 μM Cys;

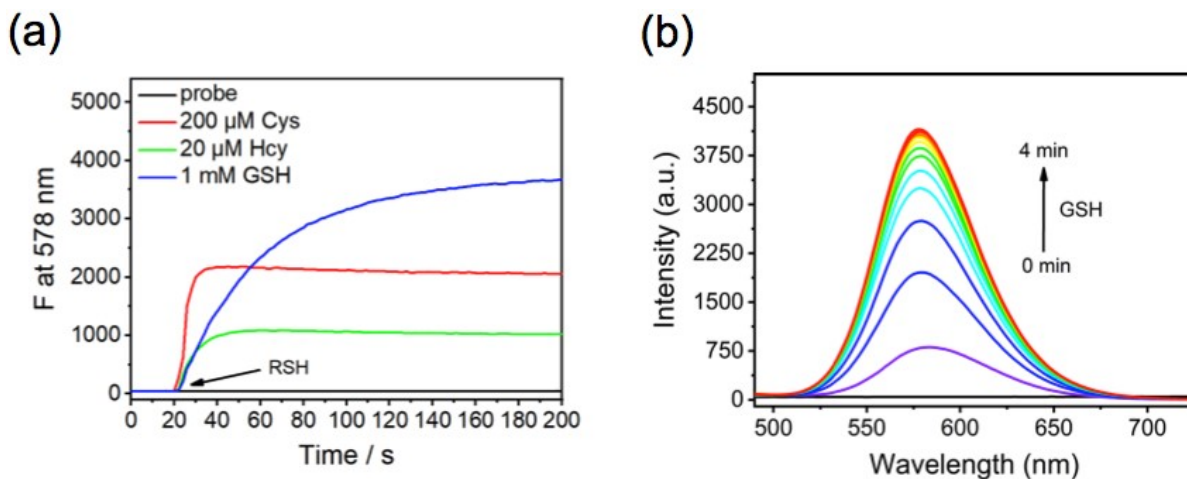
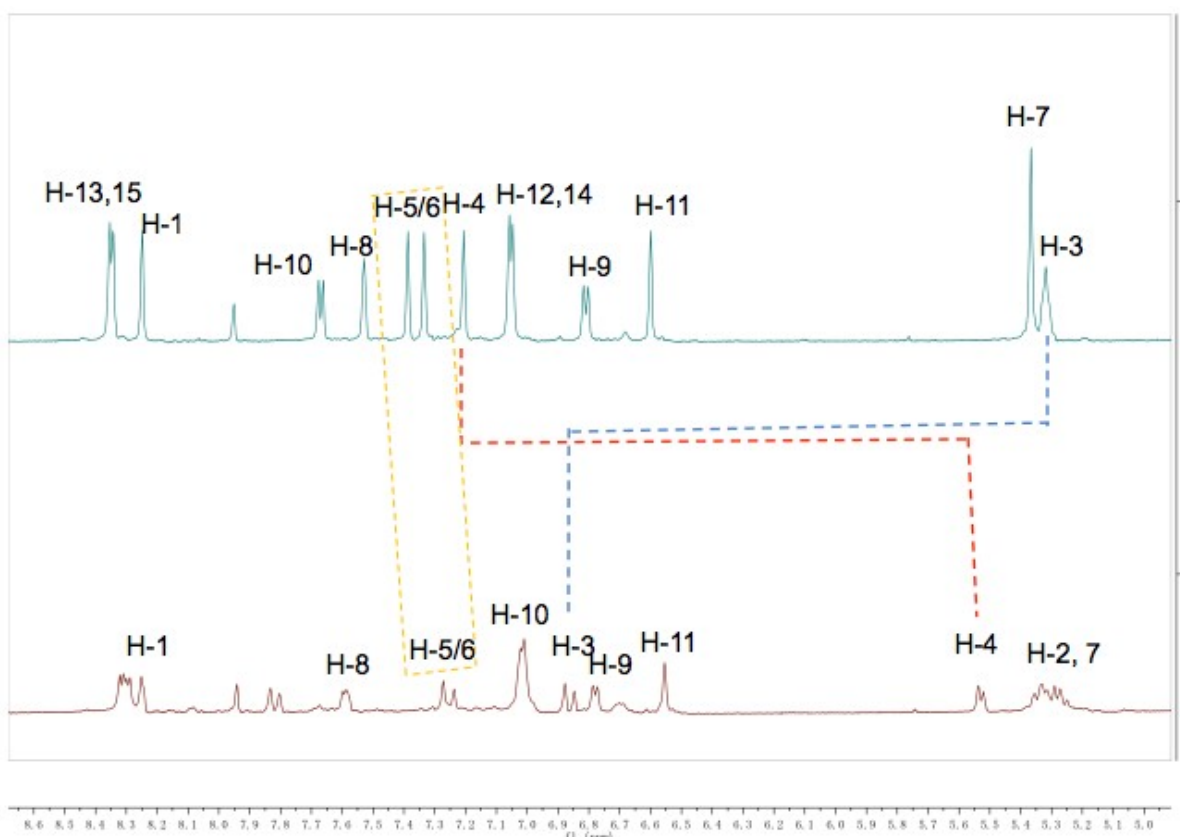


Figure S3: (a) The kinetic curve of CM-Mit (5 μM) in the mixed solvent of DMSO and PBS (1:9, v/v) without or with 200 μM Cys, 20 μM Hcy, and 1mM GSH at 578 nm. (b) The change of fluorescence spectra of probe CM-Mit (5 μM , DMSO: PBS, 1: 9, v/v) with time after the addition of 1 mM GSH



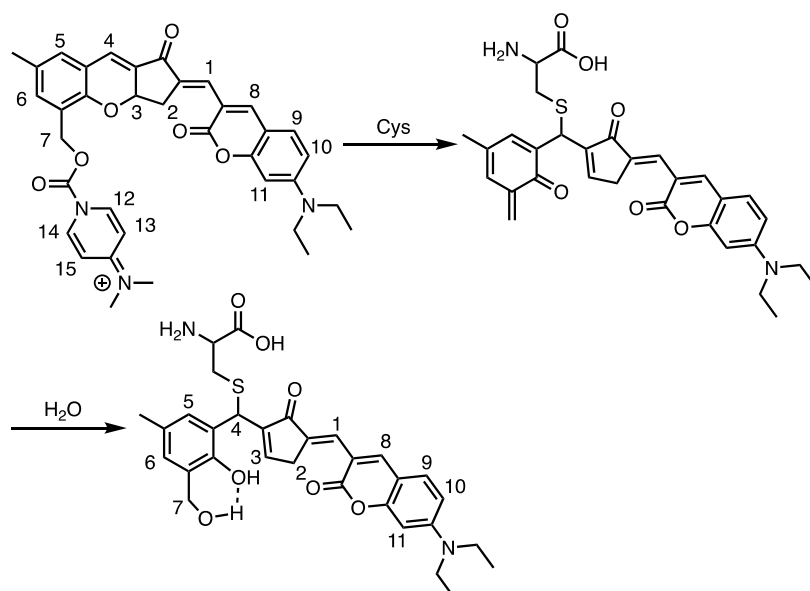


Figure S4. ¹H NMR spectral change of probe CM-Mit (1 mM) upon addition of Cys (2 mM).

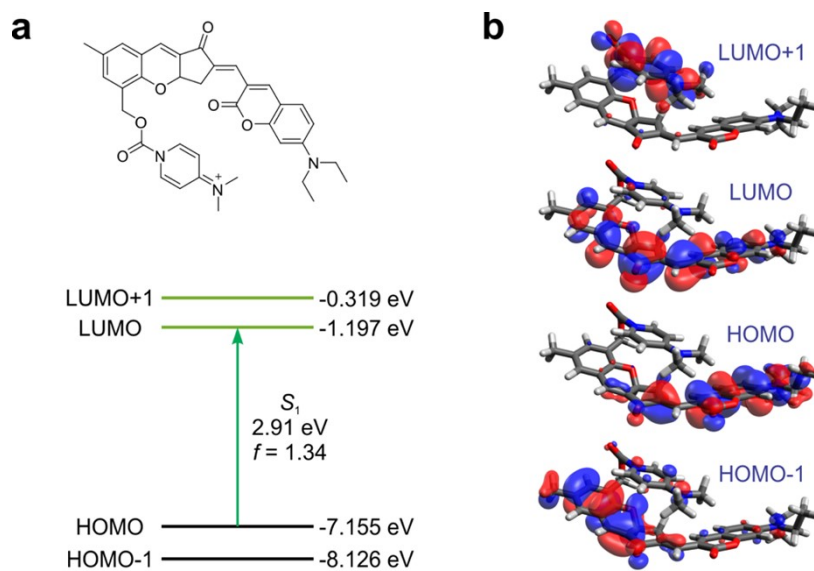


Figure S5. (a) Molecular structure and the calculated energy levels of the frontier molecular orbitals of **CM-Mit**; the inset shows the photoexcitation energy and the oscillator strength (f) during S₀→S₁ photoexcitation¹. (b) Calculated frontier molecular orbitals of **CM-Mit**.

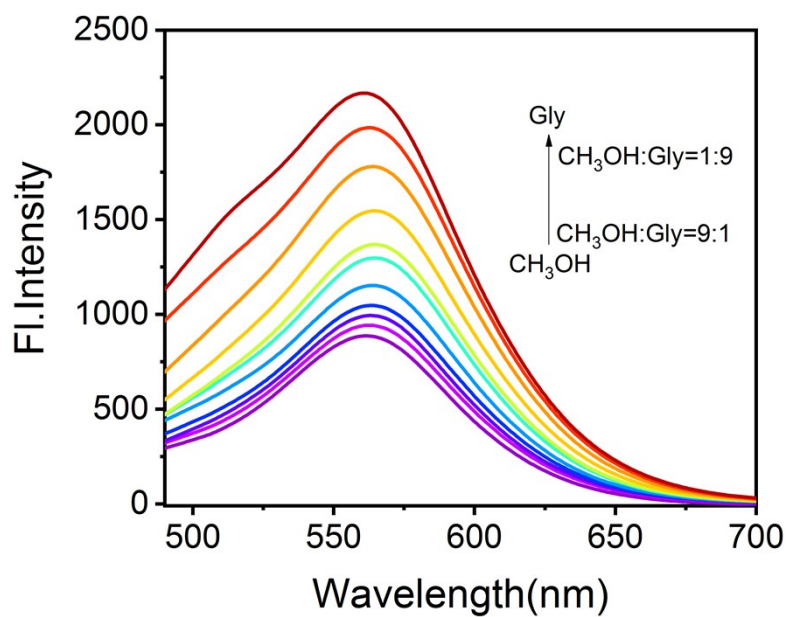


Figure S6. Studies of the intramolecular rotation process in CM-Mit.

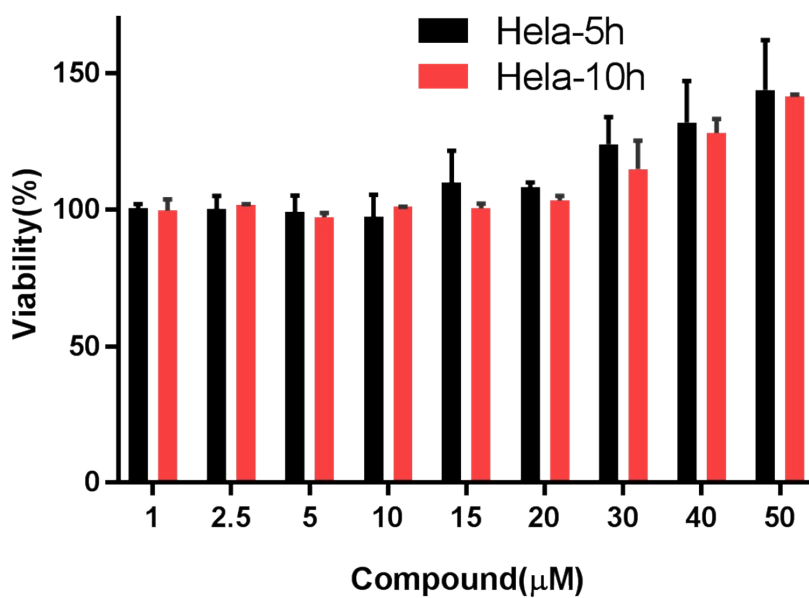


Figure S7. Cell viability values (%) estimated by MTT assay with living HeLa cell, which were cultured in the presence of 1-50 μM probe **CM-Mit** for 5 h and 10 h.

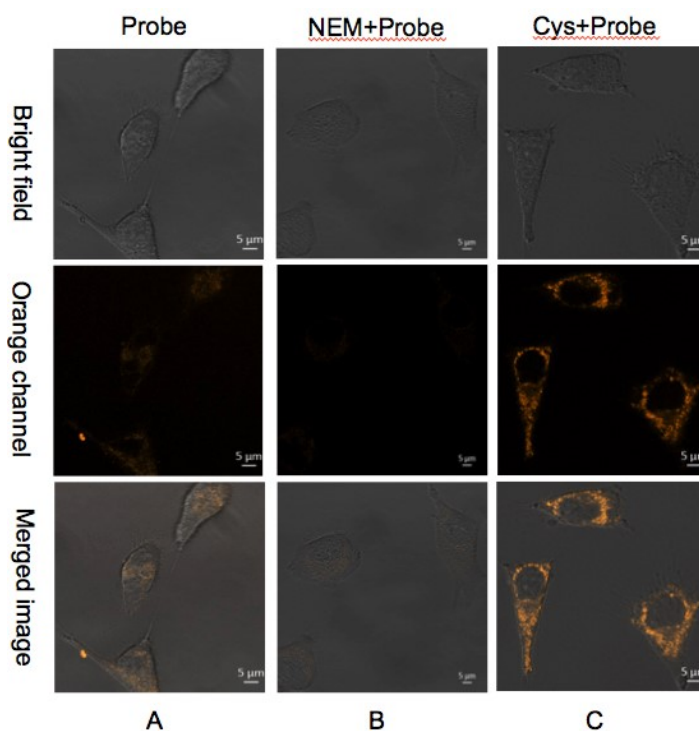


Figure S8. Fluorescence image of exogenous thiols in living HeLa cells (A–C): confocal fluorescence images of (A). HeLa cells in the presence of 10 μM of CM-Mit (B). HeLa cells were preincubated with 200 μM NEM for 20 min and then treated with 10 μM of **CM-Mit** for 10 min (C). HeLa cells were preincubated 50 μM Cys for 10 min and then treated with 10 μM of **CM-Mit** for 10 min.

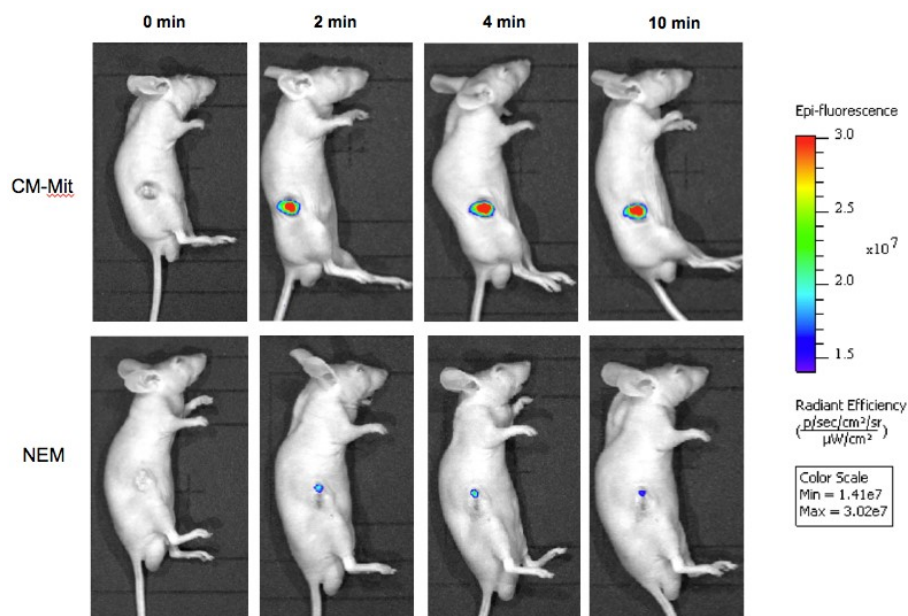


Figure S9. In vivo fluorescence imaging of mice injected with probe **CM-Mit** (a) In vivo images of mice treated with 10 μL of probe **CM-Mit** (2 mM) via tumor site injection at 0, 2, 4 and 10 min. (b) In vivo images of mice injected at the tumor site with 150 μL of NEM (1 mM) for 10 min and followed by 10 μL of probe **CM-Mit** (2 mM) at 0, 2, 4 and 10 min.

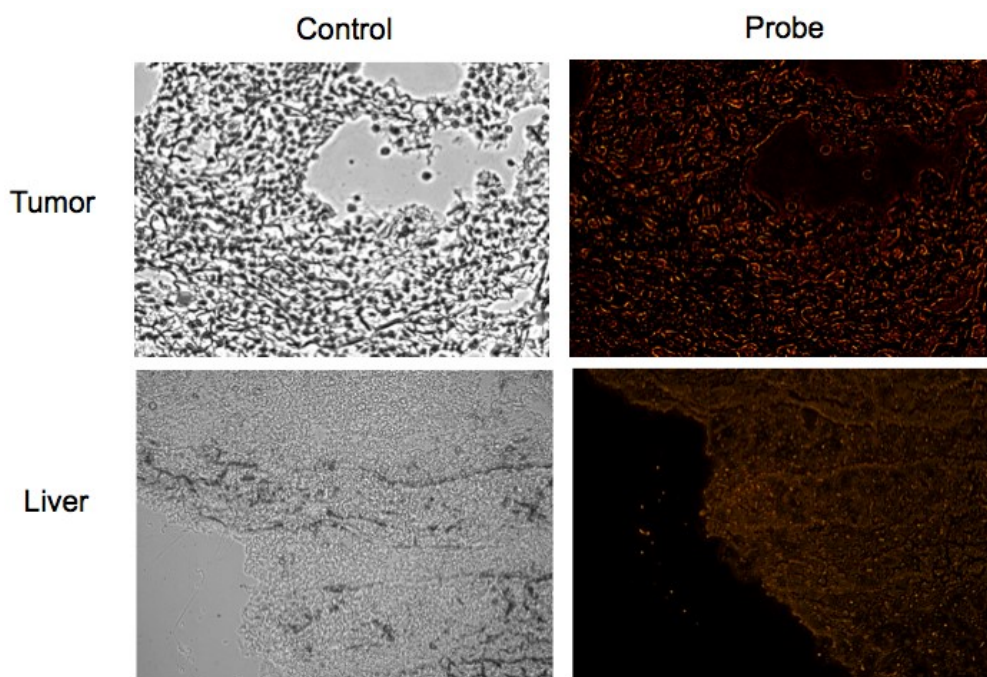


Figure S10. Representative histology of the tumor and liver of mice treated with saline and probe (50 μmol , 20 min).

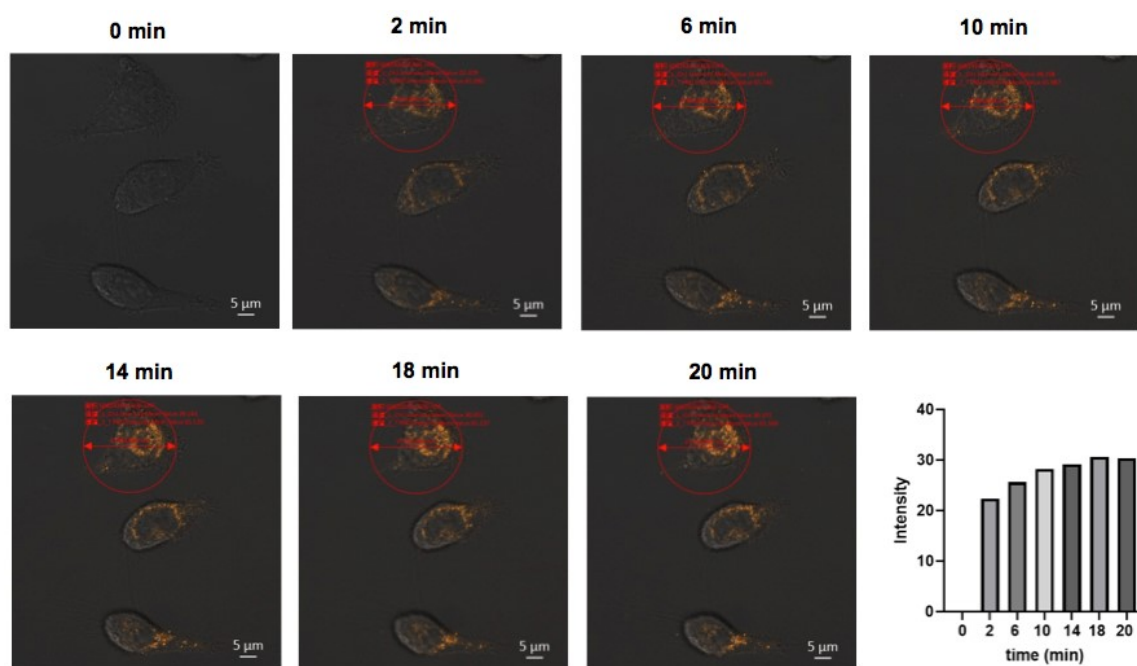


Figure S11. Fluorescence images of **CM-Mit** responding to Cys in living HeLa cells along with reaction time by confocal fluorescence

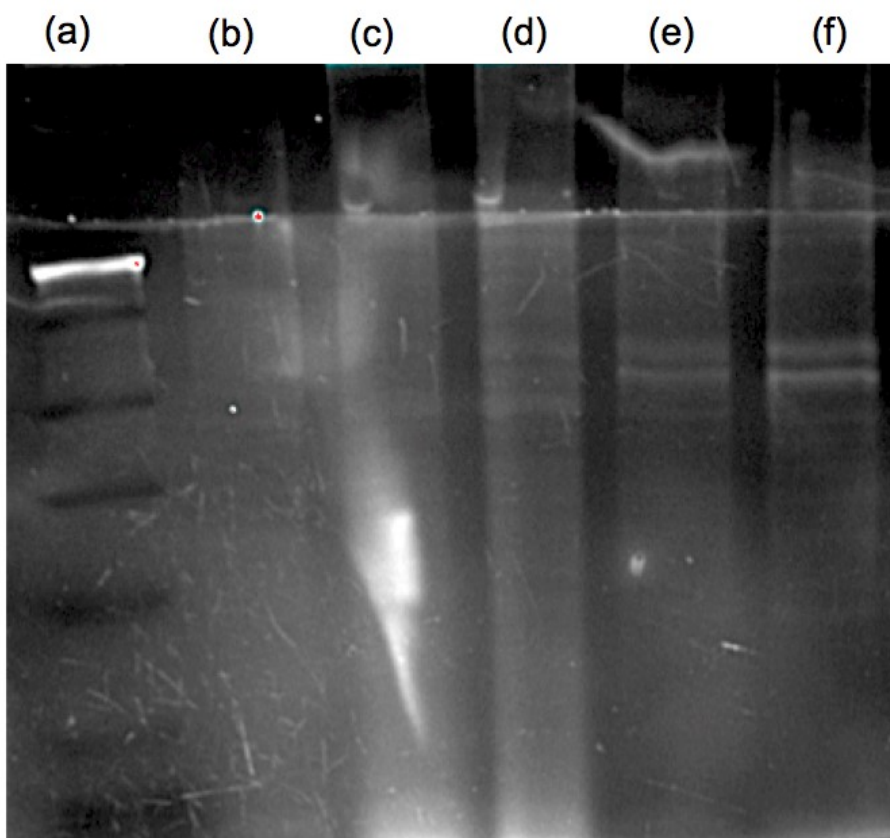


Figure S12. In-gel fluorescence. (a) Marker; (b) Cell Lysates; (c) Cell Lysates incubated with **CM-Mit** (400 μM); (d) Cell Lysates incubated with 1 mM **CM-Mit** (1 mM); (e) The cell lysates from cell incubated with **CM-Mit** (100 μM); (f) The cell lysates from cell incubated with **CM-Mit** (100 μM) and Cys (1 mM).

| | | | | |
|--------------|--------------|--|----------|----------|
| Compound No. | SA-11 | Bisdehydroneoste moninine (1) | 2 | 3 |
| Structure | | | | |
| Compound No. | 4 | 5 | 6 | 7 |
| Structure | | | | |

Table S1: The chemical structure of the *Stemona* alkaloids and their derivatives in the screening.

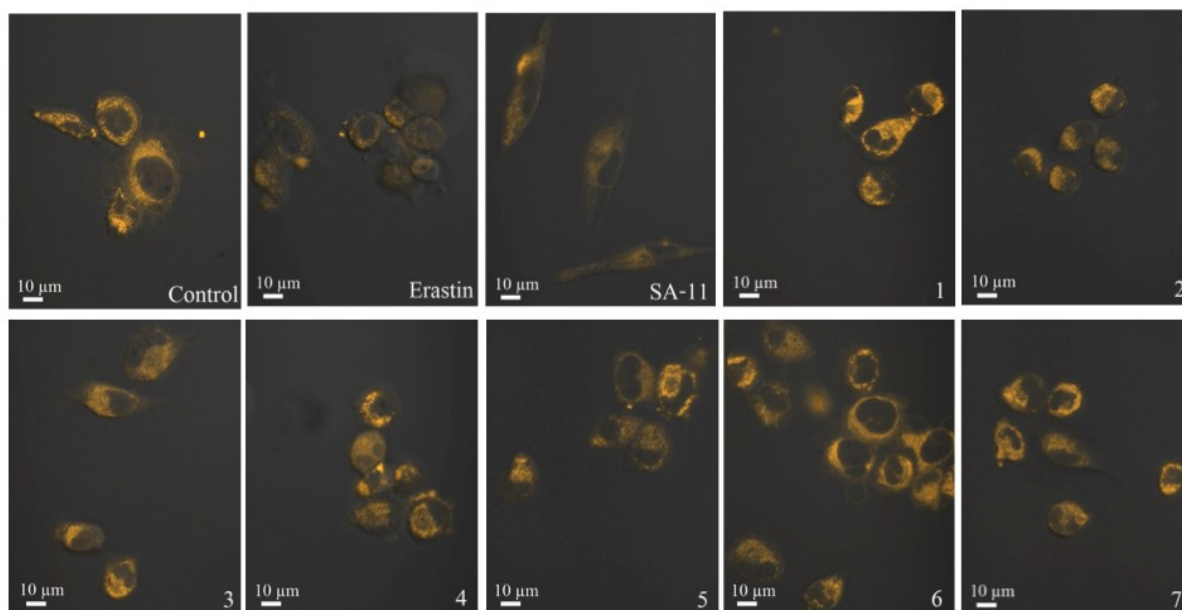


Figure S13. Screening of *Stemona* alkaloids and their derivatives for controlling the thiol level. HeLa cells were pretreated with ferroptosis inducer Erastin(5 μ M), **SA-11** and its analogue (15 μ M) in a 5% carbon dioxide incubator at 37 $^{\circ}$ C for 24 h, and followed the cells were incubated with 10 μ M **CM-Mit** for 15 min.

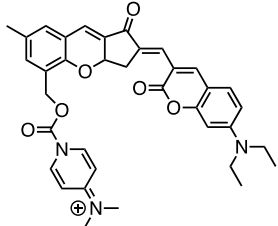
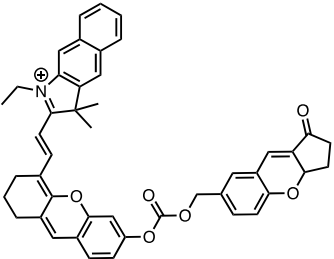
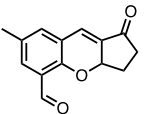
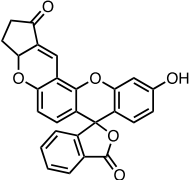
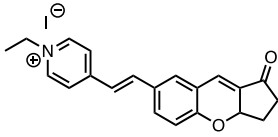
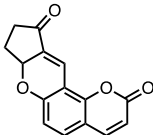
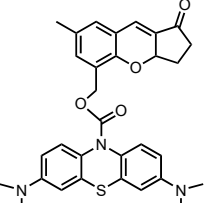
| Probes | Detection media | Ex/Em (nm) | Limit of detection | Response time | Ref. |
|---|--|------------|---|--|-----------|
|  | PBS/DMSO = 9:1 pH 7.4 | 475/578 | 0.49 μM | Cys: 10 s Hcy: 30 s GSH: 200 s | This work |
|  | PBS buffer, 30 % ethanol pH 7.4 | 645/711 | Cys: 0.39 μM Hcy: 0.54 μM GSH: 0.59 μM | Hcy: 2 min Cys: 2 min GSH: 2 min | [12] |
|  | DMSO/HEPES (v/v, 1:1, pH 7.4) | 400/515 | Cys: 64 nM | Cys: 2 min | [13] |
|  | HEPES buffer (1% CH ₃ CN, pH 7.4) | 485/520 | Cys: 50 nM Hcy: 100 nM GSH: 53 nM | unknown | [14] |
|  | PBS solution pH 7.4 | 372/496 | GSH: 3.75 μM | GSH: 1 min | [15] |
|  | HEPES buffer pH 7.4 | 362/455 | Cys: 180 nM Hcy: 820 nM GSH: 700 nM | unknown | [16] |
|  | PBS/DMSO (1:1) pH 7.4 | 600/698 | Cys: 85 nM GSH: 60 nM | Hcy: 3 min Cys: 7 min GSH: 7 min | [17] |

Table S2: Comparison of probe **CM-Mit** with other probes

NMR and MS Spectra

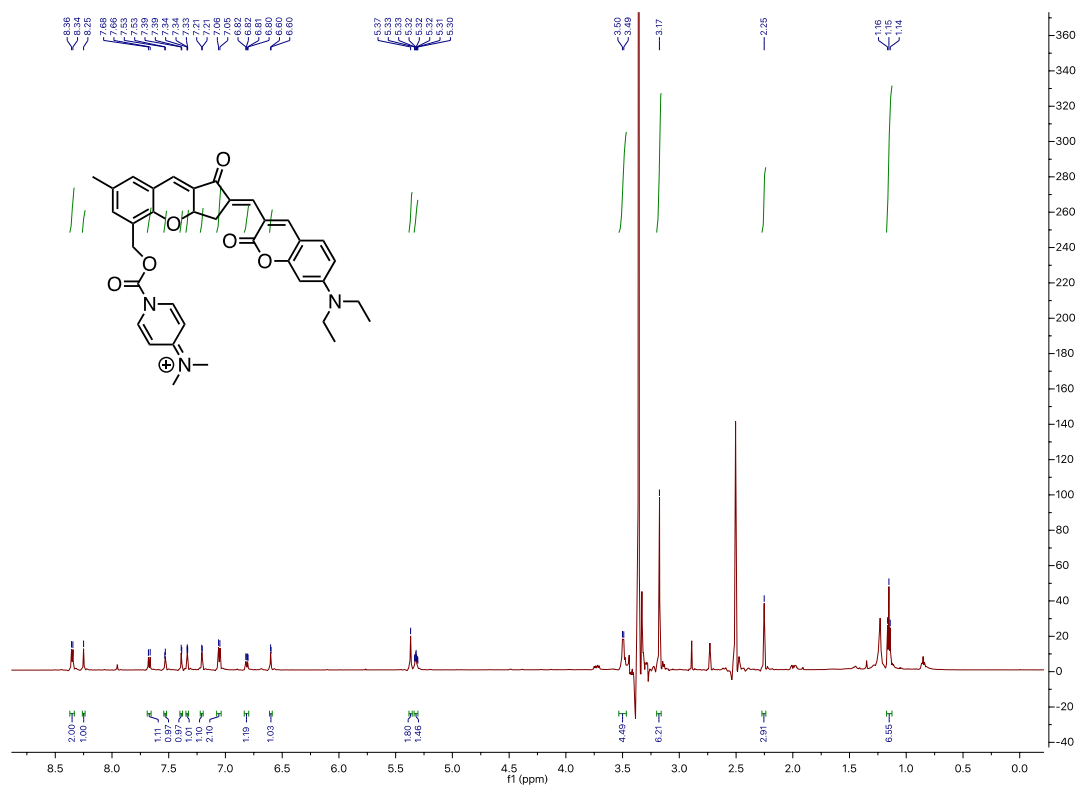


Figure S11: ^1H NMR of probe CM-Mit (600 MHz, CDCl_3)

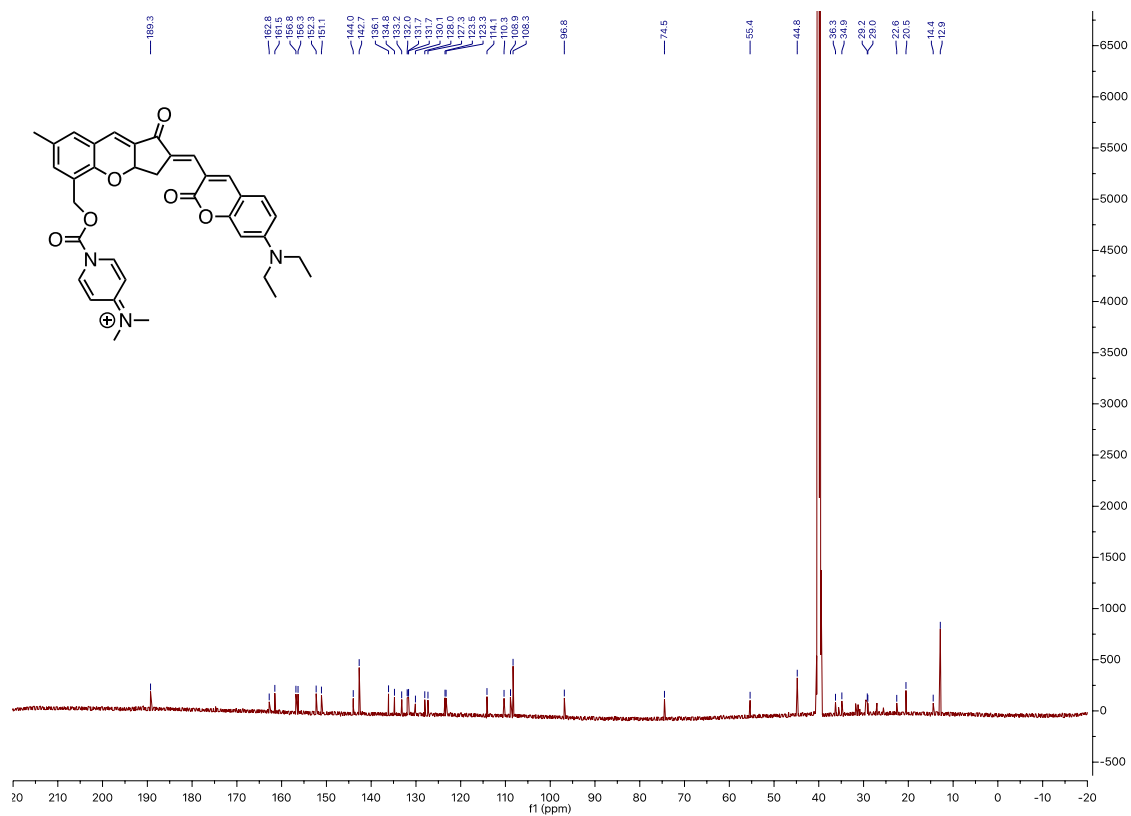
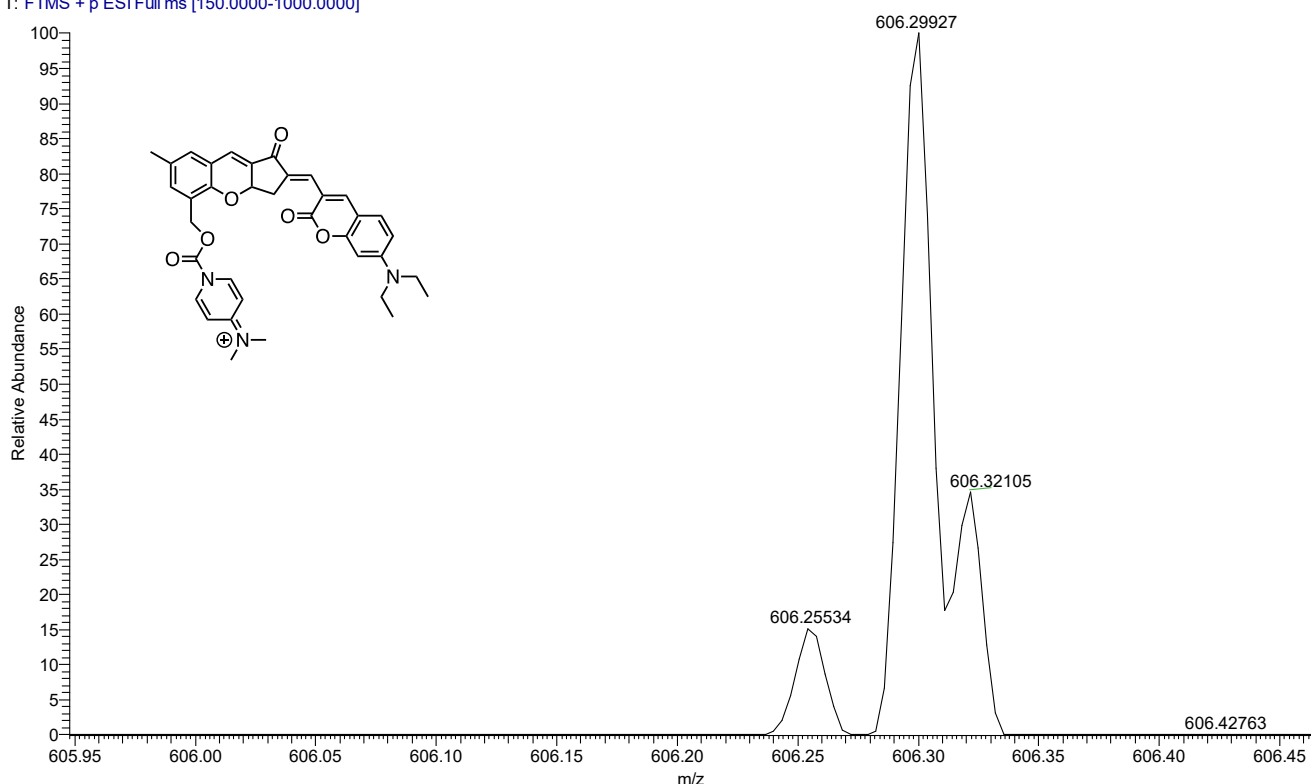


Figure S12: ^{13}C NMR of probe CM-Mit (600 MHz, CDCl_3)

YH0914-1 #5-17 RT: 0.05-0.17 AV: 7 NL: 1.85E6
T: FTMS + p ESI Full ms [150.0000-1000.0000]



HRMS (ESI) $[M + H^+]$ calculated for $C_{36}H_{36}N_3O_6$: 606.2599, found: 606.2553;

Figure S13 HRMS of probe CM-Mit

Reference:

1. K. Ma, L. Zhao, Y. Yue, F. Huo, J. Chao, C. Yin, Thiol "Click" Chromene Ring Opening and Subsequent Cascade Nucleophilic Cyclization NIR Fluorescence Imaging Reveal High Levels of Thiol in Drug-Resistant Cells, *Anal. Chem.* **2020**, *92*, 15936–15942.
2. Huo, F.-J.; Sun, Y.-Q.; Su, J.; Chao, J.-B.; Zhi, H.-J.; Yin, C.-X. Colorimetric detection of thiols using a chromene molecule. *Org. Lett.* **2009**, *11*, 4918–4921.
3. Renault, K.; Renard, P. Y.; Sabot, C., Detection of Biothiols with a Fast - Responsive and Water - Soluble Pyrazolone - Based Fluorogenic Probe. *Eur. J. Org. Chem.* **2018**, *2018*, 6494-6498.
4. Chi, W.; Chen, J.; Liu, W.; Wang, C.; Qi, Q.; Qiao, Q.; Tan, T. M.; Xiong, K.; Liu, X.; Kang, K.; Chang, Y.-T.; Xu, Z.; Liu, X., A General Descriptor ΔE Enables the Quantitative Development of Luminescent Materials Based on Photoinduced Electron Transfer. *J. Am. Chem. Soc.* **2020**, *142* (14), 6777-6785.
5. Chi, W.; Huang, L.; Wang, C.; Tan, D.; Xu, Z.; Liu, X., A unified fluorescence quenching mechanism of tetrazine-based fluorogenic dyes: energy transfer to a dark state. *Mater. Chem. Front.* **2021**, *5* (18), 7012-7021.
6. Peng, Q.; Yi, Y.; Shuai, Z.; Shao, J., Toward Quantitative Prediction of Molecular Fluorescence Quantum Efficiency: Role of Duschinsky Rotation. *J. Am. Chem. Soc.* **2007**, *129* (30), 9333-9339.
7. Becke, A. D., Density - functional thermochemistry. III. The role of exact exchange. *J. Chem. Phys.* **1993**, *98* (7), 5648-5652.
8. Scalmani, G.; Frisch, M. J.; Mennucci, B.; Tomasi, J.; Cammi, R.; Barone, V., Geometries and properties of excited states in the gas phase and in solution: theory and application of a time-dependent density functional theory polarizable continuum model. *J. Chem. Phys.* **2006**, *124* (9), 94107.
9. Frisch, M.; Trucks, G.; Schlegel, H.; Scuseria, G.; Robb, M.; Cheeseman, J.; Scalmani, G.; Barone, V.; Petersson, G.; Nakatsuji, H., Gaussian 16. Gaussian, Inc. Wallingford, CT: 2016.
10. Chai, J. D.; Head-Gordon, M., Long-range corrected hybrid density functionals with damped atom-atom dispersion corrections. *Phys. Chem. Chem. Phys.* **2008**, *10* (44), 6615-20.
11. Weigend, F.; Ahlrichs, R., Balanced basis sets of split valence, triple zeta valence and quadruple zeta valence quality for H to Rn: Design and assessment of accuracy. *Phys. Chem. Chem. Phys.* **2005**, *7* (18), 3297-3305.

9. Marenich, A. V.; Cramer, C. J.; Truhlar, D. G., Universal solvation model based on solute electron density and on a continuum model of the solvent defined by the bulk dielectric constant and atomic surface tensions. *J. Chem. Phys. B* **2009**, *113* (18), 6378-6396.
10. Caricato, M.; Mennucci, B.; Tomasi, J.; Ingrosso, F.; Cammi, R.; Corni, S.; Scalmani, G., Formation and relaxation of excited states in solution: a new time dependent polarizable continuum model based on time dependent density functional theory. *J. Chem. Phys.* **2006**, *124* (12), 124520.
11. Hanwell, M. D.; Curtis, D. E.; Lonie, D. C.; Vandermeersch, T.; Zurek, E.; Hutchison, G. R., Avogadro: an advanced semantic chemical editor, visualization, and analysis platform. *J. Cheminformatics* **2012**, *4* (1), 1-17.
12. Yang, Y.; Zhou, T.; Jin, M.; Zhou, K.; Liu, D.; Li, X.; Huo, F.; Li, W.; Yin, C. A thiol-chromene "click" reaction triggered self-immolative for NIR visualization of thiol flux in physiology and pathology of living cells and mice. *J. Am. Chem. Soc.* **2020**, *142*, 1614-1620.
13. Yue, Y.; Yin, C.; Huo, F.; Chao, J.; Zhang, Y. Thiol-chromene click chemistry: a turn-on fluorescent probe for specific detection of cysteine and its application in bioimaging. *Sens. Actuators, B* **2016**, *223*, 496-500.
14. Chen, X.; Ko, S. K.; Kim, M. J.; Shin, I.; Yoon, J., A thiol-specific fluorescent probe and its application for bioimaging. *Chem. Commun.* **2010**, *46* (16), 2751-2753.
15. Ren, W. X.; Han, J.; Pradhan, T.; Lim, J. Y.; Lee, J. H.; Lee, J.; Kim, J. H.; Kim, J. S., A fluorescent probe to detect thiol-containing amino acids in solid tumors. *Biomaterials* **2014**, *35* (13), 4157-4167.
16. Yang, Y.; Huo, F.; Yin, C.; Zheng, A.; Chao, J.; Li, Y.; Nie, Z.; Martinez-Manez, R.; Liu, D., Thiol-chromene click chemistry: a coumarin-based derivative and its use as regenerable thiol probe and in bioimaging applications. *Biosens. Bioelectron.* **2013**, *47*, 300-306.
17. Ma, K.; Zhao, L.; Yue, Y.; Huo, F.; Chao, J.; Yin, C., Thiol "Click" Chromene Ring Opening and Subsequent Cascade Nucleophilic Cyclization NIR Fluorescence Imaging Reveal High Levels of Thiol in Drug-Resistant Cells. *Anal. Chem.* **2020**, *92* (24), 15936-15942.